

Journal of Materials Chemistry A

Accepted Manuscript



This is an *Accepted Manuscript*, which has been through the Royal Society of Chemistry peer review process and has been accepted for publication.

Accepted Manuscripts are published online shortly after acceptance, before technical editing, formatting and proof reading. Using this free service, authors can make their results available to the community, in citable form, before we publish the edited article. We will replace this *Accepted Manuscript* with the edited and formatted *Advance Article* as soon as it is available.

You can find more information about *Accepted Manuscripts* in the [Information for Authors](#).

Please note that technical editing may introduce minor changes to the text and/or graphics, which may alter content. The journal's standard [Terms & Conditions](#) and the [Ethical guidelines](#) still apply. In no event shall the Royal Society of Chemistry be held responsible for any errors or omissions in this *Accepted Manuscript* or any consequences arising from the use of any information it contains.

Cite this: DOI: 10.1039/coxx00000x

www.rsc.org/xxxxxx

ARTICLE TYPE

Declined ionic flux through the nano pores of vertically aligned carbon nanotubes filled by the PNIPAm hydrogel

Yuanyuan Pan^{a,b}, Qiang Wu^{a,c}, Yuyan Weng^{a,c}, Xiaohua Zhang^{*a,c}, Zhaohui Yang^{*a,c}, Jianqiang Meng^d and Ophelia K.C. Tsui^c

5

Received (in XXX, XXX) Xth XXXXXXXXX 20XX, Accepted Xth XXXXXXXXX 20XX

DOI: 10.1039/b000000x

We demonstrate a novel nano-porous membrane of 10nm in diameter multiwall carbon nanotubes (MWCNTs) filled with thermal sensitive poly(N-isopropylacrylamide) (PNIPAm) hydrogel. The high-resolution transmission electron microscopy (HRTEM), Micro FT-IR spectroscopy and confocal laser scanning fluorescence microscopy are used to confirm the MWCNT filled with the hydrogel. An improvement in hydrophilicity of the gel-filled nano-channel is expected to promote the migration of aqueous solutions and the transportation of water. Meanwhile a decrease in ion flux is observed after the nano-pores of MWCNT are filled with hydrogel. This new hydrogel filled-CNT material shows potential for nano-chromatography, water purification and intelligent ionic channels.

Introduction

One-dimensional nanoscale cavity of carbon nanotubes (CNTs) are of particular interests because of the tiny amount of mass they store and deliver.^{1, 2} Such confinement caused by the nano pore of CNTs greatly influences molecular packing, orientation, translation and reactivity due to nano-confinement effect.³⁻⁶ The special structure of CNTs make them attractive candidates for bio-imaging, drug delivery, catalysis and photonic devices.⁷⁻¹⁰

Mass transport in the nano-channels of CNTs has also attracted much attention in biological systems. Enhanced transportation of water molecules in CNT nanopores has been observed and investigated theoretically¹¹ and experimentally^{12, 13}. A variety of strategies have been attempted to control the ionic transportation in the nano-channels of CNTs such as decreasing the CNTs diameter¹⁴, modifying the CNT ends¹⁵, and applying an external electric field¹⁶. However, the problem of implanting moieties inside the CNT nanoscale channels for the modulation of mass transportation remains a challenge.

In this work we demonstrate encapsulation of thermal-sensitive poly(N-isopropylacrylamide) (PNIPAm) hydrogel into CNT nano-channels that are 10 nm in diameter in a pre-aligned nanoporous CNT membrane. After inter-diffusion of reactants into the nano-channels then in-situ polymerization, PNIPAm hydrogel formed in the CNT channels as confirmed by high-resolution transmission electron microscopy (HRTEM), Micro FT-IR spectroscopy and confocal laser scanning fluorescence microscopy. The entrance of the CNT nano-pore becomes more hydrophilic after the formation of hydrogel which may facilitate transportation of water. The diffusion rate of KCl and Ru(bipy)₃²⁺ complex ions in the hydrogel-filled CNT nanopores decreases almost 50% as compared to the un-filled CNT nano-channel. This

result may shed light on designing high-efficient separation membrane for desalination and controllable drug release. Additionally, the fluorescence labelled hydrogel within the CNT nano-channels exhibits excellent stability during the etching treatment which may imply practical benefit to bio-imaging.

Generally, a hydrophilic hydrogel can fill or modify a hydrophilic channel having a relatively large diameter (usually larger than 30 nm), as demonstrated in track-etched polymeric membranes¹⁷, anodic aluminum oxide (AAO) templates¹⁸, or amorphous carbon nanotube.¹⁹ However it is challenging to fill a hydrophilic hydrogel into a super-hydrophobic graphitic CNT nano-channel especially when the pore diameter is below 20 nm due to the poor wettability and extremely high aspect ratio of CNTs. Herein vertically aligned CNTs with open ends which is embedded inside an epoxy matrix is used as the platform. Compared with traditional wet-filling methods *via* capillary forces, the concentration difference on the two sides of the membrane drives the reactants to diffuse into the CNT nano-channels. The epoxy resin fills all the gaps between the CNTs and eliminates the gel wrapping outside the CNTs. Our previous study showed a unique wetting-dewetting behavior of the hydrophilic hydrogel filling the outside space of superhydrophobic CNT arrays²⁰ and a dramatically enhancement of water flux through a polyether sulfone filled CNT array membrane.²¹ In this paper we will show an improved water adsorption property accompanied by a reduction in the ion-flux. These properties highlight the potential of hydrogel filled-CNT porous membranes in a wide range of applications such as nano-chromatography, drug-delivery as well as mimic of intelligent ionic channels.

Results and Discussion

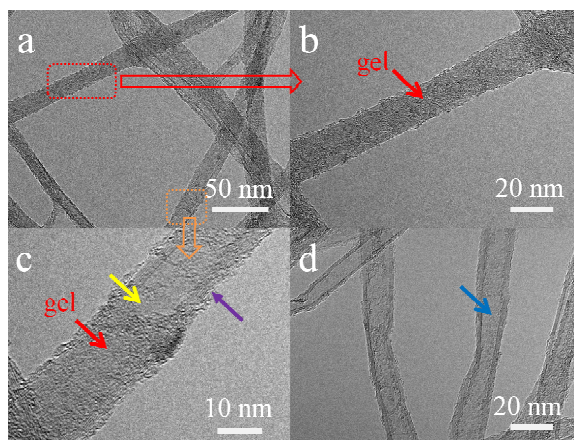


Figure 1. a) Typical TEM images of PNIPAm hydrogel filled CNTs with an inner diameter of 10 nm; 1b) magnified rectangular area of 1a indicating a hydrogel fulfilled CNT (the hydrogel part is indicated by the red arrow); 1c) magnified square area of 1a. The yellow arrow corresponds to an edge of the hydrogel and the purple arrow indicates the graphite layer of CNT; 1d) Unfilled-CNTs (the hollow channel of CNT is indicated by the blue arrow)

Figure 1a shows a representative TEM image of the PNIPAm hydrogel filled CNTs with an inner diameter of 10 nm. In comparison, the TEM image of unfilled CNTs (Fig 1d) show clearly hollow cavity structures as indicated by the blue arrow. After impregnation of the gel, the hollow cavity becomes opaque. The dark regions correspond to the gel as pointed out by the red arrow in Figure 1b. This result is similar to a previous work reported by Wu who filled gelatin inside a 40-nm diameter CNT channel within an AAO template.¹⁹ In Figure 1c, a clear curved edge of the gel interfacing with the hollow CNT cavity as indicated by the yellow arrow is observed. This may be caused by an air bubble due to the poor compatibility between the superhydrophobic inner wall of the CNTs and the hydrophilic reactant solution. The graphite layer of CNTs' external wall is clearly distinguishable from the background and filled organics (pointed out by the purple arrow in figure 1c). No significant epoxy residues wrapping the outside of CNTs are observed. The slight distortion of some graphite layers suggests damage of the CNT external walls during the strong acid etching process. The filling efficiency based on the TEM images taken is estimated to be ca. 50%. The relatively low filling efficiency is attributed to air bubbles formed during the diffusion process and the blocked nano-channels in the bamboo-like CNTs.

FT-IR spectra analysis

We next measure the micro FT-IR spectra of the un-filled CNTs and hydrogel-filled CNTs to detect the chemical composition of the infillings. Figure 2 shows the micro-FT-IR spectra of the gel-filled CNTs (curve a), unfilled CNTs (curve b) and pure hydrogel (curve c). The FT-IR spectra of un-filled CNTs samples after undergoing the same etching treatment show a peak at 1657 cm^{-1} (curve b), which comes from the carboxyl groups on the external walls of the CNTs. After gel-filling, a shoulder vibrational peaks appears at 1628 cm^{-1} (curve a), which is also found in the pure hydro-gel sample (curve c). This peak is related to the amide I

band, consisting of the C=O stretch of PNIPAm. Another characteristic peak of the gel around 1550 cm^{-1} from the N-H stretching is however not observed in the gel-filled CNT samples. It may be caused by reduction of the IR vibrational cross-section in a confined environment.²²

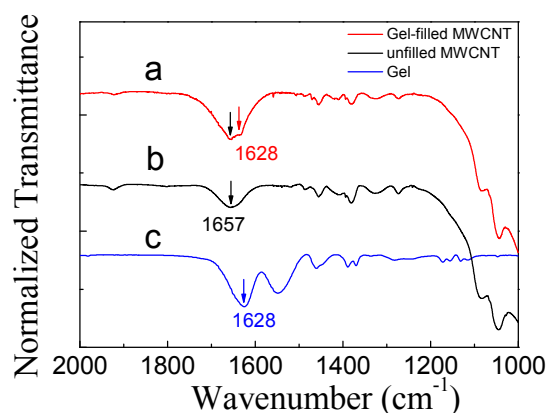


Figure 2. Micro FT-IR spectra of gel-filled CNTs (a), unfilled CNTs (b) and pure hydrogel (c)

Confocal laser scanning fluorescence microscopy

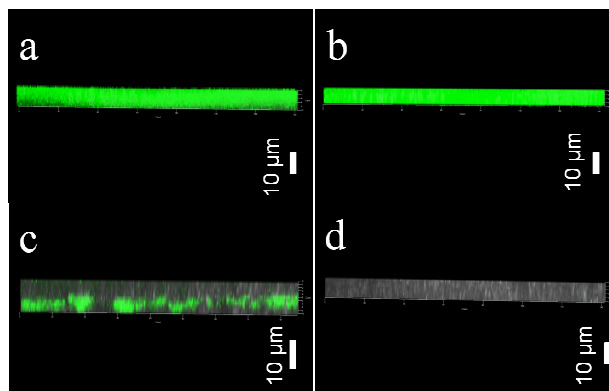


Figure 3. Confocal laser scanning fluorescence microscopy images of CdTe QDs/hydrogel@CNT samples before (a) and after immersion in a 1M H_2SO_4 solution for over 24 hr (b); CdTe dip-coated CNT membranes before (c) and after immersion in a 1M H_2SO_4 solution for 5 min (d)

To further establish the distribution of the hydrogel in the hydrogel@CNT membrane, we use fluorescent CdTe quantum dots (QDs) as probes for the whereabouts of the hydrogel. In this experiment, the CdTe QDs (2 nm in diameter) with a green emission is allowed to diffuse with the NIPAm monomer and finally get trapped within the hydrogel formed. Figure 3a shows a 3-D fluorescent image of the CdTe QDs labeled PNIPAm-filled CNT membrane. A homogeneously distributed fluorescence along the Z-axis of a CNT ($\sim 10 \mu\text{m}$) indicates an efficient filling of the CdTe QDs within the CNTs nano-channels. For comparison we also subject a CNT membrane sample to be coated by the same CdTe QDs aqueous solution. Weak and randomly distributed fluorescence signals are observed along the Z-axis within 3 μm depth as shown in Figure 3c. It indicates that the CdTe QDs cannot diffuse into the epoxy matrix but are adsorbed onto the CNT surface. Next, we compare the emission

stability of the CdTe QDs encapsulated inside the gel-filled CNTs to that of the QDs in a free state. As shown in Figure 3b, the membrane of CdTe QDs labeled gel-filled CNTs maintains a strong emission even after submersion in a bleaching solution of 1M H₂SO₄ for over 24 hr. On the other hand, the fluorescence of the CdTe QDs coated on the interface between the CNT and the epoxy resin is thoroughly quenched within 5 min as shown in figure 3d. This result suggests that CNT encapsulation can protect CdTe QDs from the acid quenching. This unique character of gel@CNT shows a potential application for bio-imaging.

Contact angle measurements

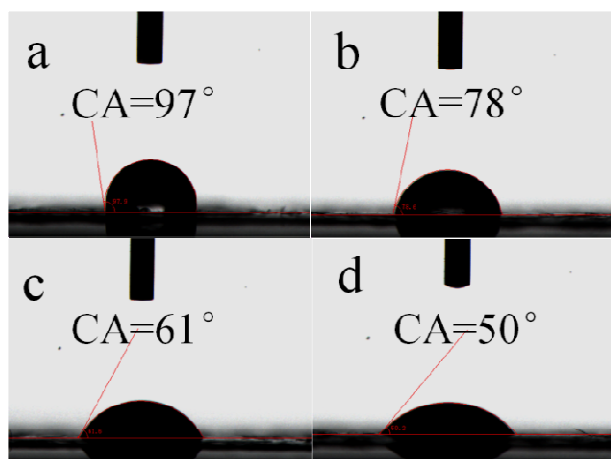


Figure 4. CCD photographs showing the contact angle measurement of a water drop resting on a) an as-microtome-cut CNT porous membrane; b) a CNT porous membrane after the O₂ plasma etching treatment; c,d) the CNT membrane after hydro-gel infilling (c, with the membrane facing monomer side up; d, with the membrane facing initiator side up)

Next, we investigate the surface wettability of the CNT nanoporous membrane before and after the gel-infiltration, a factor that can influence mass transportation in the CNT nano-channel. Figure 4a and 4b shows the water contact angle of the CNT/epoxy nano-porous membrane at 21°C before and after plasma etching, respectively. A contact angle of $97 \pm 2^\circ$ (figure 4a) indicates that the surface of the as-cut CNT membrane is super-hydrophobic. Plasma etching can improve its hydrophilicity by introducing some polar groups (such as carboxylic or carbonyl groups) to the entrance of the CNTs, as confirmed by the smaller contact angle of $78 \pm 2^\circ$ (figure 4b) found after etching. The hydrophilicity of the same membrane surface is further improved after hydrogel-encapsulation, as indicated by further reduction in the water contact angle of the surface facing the monomer solution ($61 \pm 3^\circ$, figure 4c) and the surface facing the initiator solution ($50 \pm 2^\circ$, figure 4d), respectively. The smaller water contact angle of the surface facing the initiator may be caused by the larger amount of sulfate groups (generated by the initiators) in the gel. This improved hydrophilicity of the membrane may facilitate the up-take of aqueous solution by and water transportation through the membrane. A point should be noted about the water contact angle measurements found here of the hydrogel-filled MWCNTs nanopores relative to those of the empty ones we found before.²⁰ In this work, the water contact angle is somewhat bigger than the value reported in our previous paper (about 12°). This increase in

contact angle is due to the significantly smaller weight percentage of hydrogel in the CNT channels than between the CNT interspaces.

Ion diffusion Test

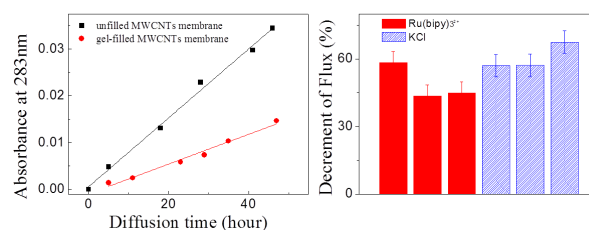


Figure 5. a) The UV-vis absorbance at 283 nm of the Ru complex ions in the permeate part versus diffusion time before (squares) and after gel infiltration (circles); b) Ion flux decrement of Ru complex ions (solid) and KCl (stripe pattern) through different gel-filled CNT nano-porous membranes. Each test is repeated three times with a new membrane used in each experiment.

The diffusion behavior of ions in an unfilled CNTs nanopore with the diameter larger than 7 nm has been found to be similar to that of free ions.²³ After the gel infiltration a reduction in the ion flux is observed due to blockage of the nano-pores. TEM images (figure 1a-c) show no obvious gaps between the gel and the CNT inner wall. It indicates that the ions diffuse in the confined gel matrix. Figure 5a shows the UV-vis absorbance at 283 nm of the Ru complex ions in the permeating solution versus diffusion time before and after gel infiltration. From the linear relationship seen between the absorbance and diffusion time, we can conclude that the diffusion rate of Ru ions in the hydrogel-filled CNTs membrane decreases by almost 50% as compared to that in an otherwise identical un-filled CNT membrane. A similar reduction is also observed in the diffusion rate of KCl ions through the membranes after the PNIPAM hydrogel impregnation. As shown in figure 5b the decrease in the diffusion rate is $49\% \pm 5\%$ and $60\% \pm 6\%$ for Ru(bipy)₃²⁺ and KCl, respectively. The variations are caused by the different filling efficiency and interactions between the ions and the gel.

We also check the long-term transportation stability of the gel-filled CNT membranes. There are no obvious changes on the ion transportation speed after 72-hours diffusion due to the crosslinked structure of the hydro-gel.

There are on-going studies examining further ion diffusion and physical properties of the gel confined inside the CNT channels at different temperatures. Future studies will investigate 'intelligent' ion channels made of other chemical or pH-responsive hydrogel modified CNT nano-channels.

Experimental Section

Materials

The N-isopropyl acrylamide (NIPAm) monomer, Polyethylene glycol (PEG-600), N,N,N',N'-tetramethylethylenediamine (TMEDA), N,N'-methylene bisacrylamide (MBAA) (the cross-linking agent) and ammonium peroxydisulfate (the initiator), were purchased from Sinopharm Chemical Reagent Co., Ltd. without further purification. The SPI-Pon-812 monomer, curing agents dodecyl succinic anhydride (DDSA) and 5-norbornene-

methyl-2,3-dicarboxylic anhydride (NMA), dimethylaminomethyl phenol (DMP-30) as accelerator were supplied by SPI Supplies, Division of Structure Probe Inc. Au colloidal dispersion (20 nm in diameter) from Ted Pella Inc. with size distribution less than 5% was used to check the gaps between the CNTs and epoxy matrix. Other chemicals are supplied by Sinopharm Chemical Reagent Co., Ltd. without further purification. Water-dispersible CdTe quantum dots (2 nm in diameter) with green emission were synthesized using a method reported previously.²⁴ The DI water (>18 MΩ) was used as the solvent for all experiments.

Characterization

TEM images were obtained by using a Tecnai G²20 (FEI) microscope at 200 KV accelerating voltage. The isolated MWCNTs were firstly released from the epoxy matrix through an acid digestion process. Then it was dispersed in an ethanol solution and drop-coated onto a copper grid for TEM test. The scanning electron microscopic (SEM) pictures were taken with a Hitachi S-4700 (Hitachi Inc.) SEM. The Epoxy-embedded MWCNT array membrane samples were first quenched in a liquid nitrogen. The chips were mounted onto the sample stage with a Cu paste to capture the cross-section images of the MWCNT/epoxy composite membrane. Confocal laser scanning fluorescence microscopy (LSM710, Zeiss) was used to determine the spatial distribution of the fluorescence-labeled hydrogel within the CNT nano pores by recording a 3-D fluorescence image of a sliced membrane mounted on a clean slide glass at an ambient condition. Contact angle(CA) measurement was carried out on a contact angle goniometer (OCA20, Dataphysics, Germany) equipped with a video camera at 21°C to check the hydrophilicity of the membrane surface. The gel-filled MWCNT membrane was first rinsed by DI water for three times and then dried in the air overnight before the CA measurement. Micro FT-IR spectra are obtained from a Nicolet 6700 FT-IR spectrophotometer by testing the isolated MWCNT samples released from the epoxy matrix after acid etching.

Preparation of nano-porous CNT membrane

Vertically aligned CNT arrays having a height in the range of 0.1 - 1 mm and an inner diameter of 10 ± 2 nm are synthesized through a traditional chemical vapour deposition (CVD) method.²⁵ A 10µm-thick CNT/epoxy composite film was obtained by using a microtome-cut. We etch the membrane by O₂ plasma to remove the organics around the CNT tips prior to diffusing solution into the CNT nano-channels. Details are provided in the supporting information and our previous work.^{25, 26}

Encapsulation of PNIPAm hydrogel inside CNTs

The CNT nano porous membrane is first placed between two silicone pads in a diffusion cell (Figure S1c, supporting information). The feeding cell contains 5 mL of the degassed NIPAm monomers (1M), PEG-600 (0.2M) and cross-linking agent MBAA (0.2M) in a mixed solution (mH₂O:mEtOH = 4:1). The cell on opposite side contains 5 mL of the mixed solution (mH₂O:mEtOH = 4:1). After 72 hours of diffusion, the initiator (NH₄)₂S₂O₈ (0.2M) and accelerator TMEDA(60uL) were added to the permeate side and feeding side, respectively. The PNIPAm is formed within the CNT nano channels via in-situ

polymerization under ambient conditions after 48 h. The as-prepared membrane is thoroughly washed using DI water and then soaked in DI water over 3 days until no significant change in conductivity is observed (The DI water is changed every 8 hours). In order to remove the epoxy matrix, an acid etchant containing concentrated sulfuric acid and hydrogen peroxide (2:1 in volume) was used to dissolve the epoxy at 90°C for 5 days. The PNIPAm@CNT was filtered using a PTFE membrane (10µm pore size) and thoroughly washed with DI water.

Ion diffusion Test

KCl ions are usually used as the probes to measure the ion-flux behavior of a nano-channel because the diffusion coefficient of K⁺ and Cl⁻ is quite close which will eliminate the liquid junction potential. Also the Ion flux is easy to monitor by conductivity measurements.^{12, 23}

All the diffusion tests are carried out at 21 ± 1°C. The feed solution contains 5 ml of 1200 µS of KCl solution and that on the permeate side is 5 ml 70 µS of KCl. The conductivity of the permeate side solution is monitored by a water analyzer (Ultrameter II, Myron L Company) and the data is collected every 2 hours. The conductivity meter is calibrated using a 66.9 ppm standard solution before the experiment.

The diffusion rate of KCl can be obtained by measuring the conductivity change in the solution on the permeate side. Since mass diffusivity is related to the pore size of the CNTs, the efficient permeable pore area (A_{eff}) can be calculated from the equation below:¹²

$$A_{eff} = \Delta C \times h \times V_p / (D \times C_f \times t), \quad (1)$$

where D is the bulk diffusivity of KCl at 21°C ($1.96 \times 10^{-5} \text{ cm}^2 \text{ s}^{-1}$), C_f is the conductivity of the feed (µS), h is the membrane thickness (10 µm), ΔC is the conductivity variation of the permeate (µS), t is the diffusion time (s), V_p is the permeate volume(5ml). The efficient permeable pore density can be calculated from equation (2) as follows:

$$\text{Permeable pore density (cm}^{-2}\text{)} = (A_{eff}/A_m)/(\pi d^2/4), \quad (2)$$

where, d is the average CNT pore diameter (10 ± 2 nm), and A_m is the membrane area (0.12 cm²).

Except the KCl ions, Ru complex ions have a bigger volume which may show a more obvious hindered diffusion effect. The feeding solution contains 2 mM Ru(bipy)₃Cl₂ and 0.1 M KCl. The solution on the permeate side contains 0.1 M KCl. The concentration of the Ru ions is obtained from the UV-vis absorbance of the Ru complex solution at the wavelength of 283nm (The standard absorbance curve of the Ru ions is given in Fig S3). The experiments were repeated at least three times so as to obtain proper sampling statistics.

Conclusions

In conclusion, we prepared a novel nano-porous membrane containing PNIPAm hydrogel encapsulated inside CNTs channels with a small diameter of 10 nm. Infiltration of the hydrogel inside the CNT nano-channels is confirmed by HRTEM, micro FT-IR spectroscopy and confocal laser scanning fluorescence microscopy. The hydrogel-filled CNT porous membrane shows an improved hydrophilicity and a decrease in diffusion rate for KCl and Ru complex ions. These findings demonstrate the potential of gel-filled CNT composite nano-porous membrane in

a variety of practical applications, including transportation and separation of minute amount of mass, drug delivery and mimic of intelligent ionic channels.

Acknowledgements

This work was financially supported by the National Basic Research Program of China (973Program) (No. 2012CB821505), National Natural Science Foundation of China (No. 21204059, 21204058, 21274103, 21104054), Natural Science Foundation of Jiangsu Province (No. BK2011300). The authors also thank the Specially-Appointed Professor Plan in Jiangsu Province (No.SR10800312) and Project for Jiangsu Scientific and Technological Innovation team (2013). O. K. C. T. acknowledges support of the National Science Foundation (DMR-1310536). Prof. F. Zhu-ge, Mr. B. Fu from Ningbo Institute of Materials Technology & Engineering (Chinese Academy of Sciences), Mr. L. Li from ULVAC (Suzhou) Co., LTD are also greatly acknowledged for the help on the E-beam evaporation experiment.

Notes and references

- a. Center for Soft Condensed Matter Physics and Interdisciplinary Research, Soochow University, Suzhou, 215006, P.R. China
- b. Department of Polymer Science and Engineering, College of Chemistry, Chemical Engineering and Materials Science, Soochow University
- c. College of Physics, Optoelectronics and Energy, Soochow University
- d. Tianjin Polytech Univ, State Key Lab Hollow Fiber Membrane Mat & Proc, Tianjin 300387
- e. Physics Department, Boston University, Boston, MA, 02134
E-mail: yangzhaohui@suda.edu.cn; zhangxiaohua@suda.edu.cn

Electronic Supplementary Information (ESI) available: Preparation of MWCNT membrane, details of the ion diffusion test, SEM images of the MWCNT array and the membrane, photographs of the diffusion cell, UV-vis spectra of the Au nano-particles diffusion test and the standard absorbance curve of Ru ions are included as the supporting information shown here. See DOI: 10.1039/b000000x/

Notes

This work is dedicated to Professor Weixiao Cao, Peking University, China, for his 80th birthday in November 2014.

1. P. M. Ajayan, S. Iijima, *Nature* 1993, **361**, 333.
2. D. Ugarte, T. Stockli, J. M. Bonard, A. Chatelain, W. A. de Heer, *Applied Physics A-Materials Science & Processing* 1998, **67**, 101.
3. K. Koga, G. T. Gao, H. Tanaka, X. C. Zeng, *Nature* 2001, **412**, 802.
4. Z. W. Liu, Y. Bando, M. Mitome, J. H. Zhan, *Phys. Rev. Lett.* 2004, **93**, 095504.
5. S. Chen, G. Wu, M. Sha, S. Huang, *J. Am. Chem. Soc.* 2007, **129**, 2416.
6. V. C. Holmberg, M. G. Panthani, B. A. Korgel, *Science* 2009, **326**, 405.
7. S.Y. Hong, G. Tobias, K. T. Al-Jamal, B. Ballesteros, H. Ali-Boucetta, S. Lozano-Perez, P. D. Nellist, R. B. Sim, C. Finucane, S. J. Mather, M. L. H. Green, K. Kostarelos, B.G.Davis, *Nat. Mater.* 2010, **9**, 485.
8. S. Hampel, D. Kunze, D. Haase, K. Kraemer, M. Rauschenbach, M. Ritschel, A. Leonhardt, J. Thomas, S. Oswald, V. Hoffmann, B. Buechner, *Nanomedicine* 2008, **3**, 175.
9. X. Pan, Z. Fan, W. Chen, Y. Ding, H. Luo, X. Bao, *Nat. Mater.* 2007, **6**, 507.

10. M. A. Loi, J. Gao, F. Cordella, P. Blondeau, E. Menna, B. Bartova, C. Hebert, S. Lazar, G. A. Botton, M. Milko, C. Ambrosch-Draxl, *Adv. Mater.* 2010, **22**, 1635.
11. S. Joseph, N. R. Aluru, *Nano Lett.* 2008, **8**, 452.
12. M. Majumder, N. Chopra, R. Andrews, B. J. Hinds, *Nature* 2005, **438**, 44.
13. J. K. Holt, H. G. Park, Y. M. Wang, M. Stadermann, A. B. Artyukhin, C. P. Grigoropoulos, A. Noy, O. Bakajin, *Science* 2006, **312**, 1034.
14. Fornasiero, F.; Park, H. G.; Holt, J. K.; Stadermann, M.; Grigoropoulos, C. P.; Noy A.; Bakajin, O. *Proc. Natl. Acad. Sci. USA* 2008, **105**, 17250-17255.
15. M. Majumder, N. Chopra; B. J. Hinds, *J. Am. Chem. Soc.* 2005, **127**, 9062.
16. J. Wu, K. Gerstandt, H. Zhang, J. Liu, B. J. Hinds, *Nat. Nanotech.* 2012, **7**, 133.
17. H. Alem, A.S. Duwez, P. Lussis, P. Lipnik, A. M. Jonas, S. Demoustier-Champagne, *J. Membr. Sci.* 2008, **308**, 75.
18. P.F. Li, R. Xie, J.C. Jiang, T. Meng, M. Yang, X.J. Ju, L. Yang, L.Y. Chu, *J. Membr. Sci.* 2009, **337**, 310.
19. C.H.Wu, C. Cao, J. H. Kim, C.H. Hsu, H. J. Wanebo, W. D. Bowen, J. Xu, J. Marshall, *Nano Lett.*, 2012, **12**, 5475.
20. Z. Yang, Z. Cao, H. Sun, Y. Li, *Adv. Mater.* 2008, **20**, 2201.
21. S. Y. Li, G. M. Liao, Z. P. Liu, Y. Y. Pan, Q. Wu, Y. Y. Weng, X. H. Zhang, Z.H. Yang, O. K. C. Tsui, *J. Mater. Chem. A* 2014, **2**, 12171.
22. D. V. Kazachkin, Y. Nishimura, H. A. Witek, S. Irle, E. Borguet, *J. Am. Chem. Soc.* 2011, **133**, 8191.
23. B. J. Hinds, N. Chopra, T. Rantell, R. Andrews, V. Gavalas, L. G. Bachas, *Science* 2004, **303**, 62.
24. Z.H. Yang, L.L. Yang, S. Bai, Z.F. Zhang, W.X. Cao, *Nanotechnology* 2006, **17**, 1895.
25. G. Liao, Y. Pan, Q. Wu, S. Li, Y. Weng, X. Zhang, Z. Yang, J. Guo, M. Chen, M. Tang, O. K. C. Tsui, *Nanoscale* 2014, **6**, 14872.
26. Z. Liu, G. Liao, S. Li, Y. Pan, X. Wang, Y. Weng, X. Zhang, Z. Yang, *J. Mater. Chem. A* 2013, **1**, 13321.

Graphical Abstracts

